

## EXPERIMENTAL AND CFD MODELING OF A BENCH-SCALE GTL PACKED-BED REACTOR BASED ON FE/CU CATALYST

Mohammad Irani

*Research Institute of Petroleum Industry (RIPI), Tehran, Iran.*

Received November 24, 2013, Accepted February 10, 2014

---

### Abstract

An experimental and computational fluid dynamic (CFD) investigation was carried out to intensify the production of gasoline in a bench-scale Fischer–Tropsch Synthesis (FTS) process. A cylindrical reactor with one preheating and one reaction zone was employed. The reactor temperature was controlled using a heat jacket around the reactor's wall and dilution of the catalyst in the entrance of the reaction zone. An axi-symmetric CFD model was developed and the non-ideality of the gas mixture was considered using Peng-Robinson equation of state. A kinetic model based on 25 chemical species and 23 reactions was utilized. The model was validated against experimental measurements and the validated model was employed to investigate the effects of operating conditions on the performance of the reactor. The optimum values of operating conditions including pressure, reactor temperature, GHSV and H<sub>2</sub>/CO ratio was determined for maximum reactor performance.

**Keyword:** Fischer–Tropsch Synthesis; GTL, fixed bed reactor; Nano Fe Catalyst; CFD.

---

### 1. Introduction

The conversion of syngas (CO + H<sub>2</sub> mixtures) into liquid fuels via Fischer–Tropsch synthesis (FTS) has attracted much attention in the recent years. The increase in global energy demand, existence of numerous gas reservoirs in remote areas and the high price of crude oil in comparison to natural gas, are the main reasons of the increasing attention to FTS. In addition, converting of associated gases are appealing due to economic and environmental reasons. Also, GTL products are almost free of sulfur and aromatic hydrocarbons. Composition of the obtained products depends on the employed catalysts and operating conditions [1-2]. Numerous researches have been carried out to understand, model and optimize this process. Butt *et al.* [3] prepared and characterized Fe and Fe-Co catalysts on ZSM-5 support for FTS. Schulz *et al.* [4] investigated the selective conversion of syngas to gasoline on iron/HZSM5 catalysts. The effects of temperature, space velocity, CO/H<sub>2</sub> feed ratio and pressure on the activity of a Co/HZSM5 zeolite bifunctional catalyst were experimentally investigated by Calleja *et al.* [5]. The fixed-bed FT process, being one of the most competing reactor technologies, occupies a special position in FTS industrial processes [6].

Liu *et al.* [7] developed a two-dimensional heterogeneous model for simulation of steady and unsteady behavior of a fixed bed FTS reactor. They also reported [8] the effects of feed temperature, flow rate and the wall temperature on the steady state behavior of the reactor. Wang *et al.* [9] developed a one-dimensional heterogeneous model to predict the performance of fixed-bed Fischer–Tropsch reactors. Rahimpour *et al.* [10] proposed a novel combination of fixed-bed and slurry bubble column membrane reactor for Fischer–Tropsch synthesis. In the first catalyst bed, the synthesis gas is partially converted to hydrocarbons in a water-cooled fixed bed reactor. In the second bed which is a membrane assisted slurry bubble column reactor, the heat of reaction is used to preheat the feed synthesis gas to the first reactor. The membrane concept is suggested to control hydrogen addition. They utilized a one-dimensional packed-bed model for simulation of fixed-bed reactor. A one-dimensional model with plug flow pattern for gas phase and an axial dispersion pattern for liquid-solid suspension was used for modeling of slurry bubble column reactor. They claimed that their proposed reactor system gives favorable temperature profile and higher, gasoline yield, H<sub>2</sub> and CO conversion as well as selectivity. However, they admitted that experimental proof of concept is needed to establish the validity and safe operation of the proposed

reactor. Nakhaei Pour *et al.* [11] developed a kinetic model for water-gas-shift (WGS) reaction over a Fe/Cu/La/Si catalyst under Fischer–Tropsch synthesis (FTS) reaction condition. By comparing the results of four different models over a wide range of reaction conditions, they found that WGS rate expressions based on the formate mechanism best fit the experimental data. Although the reaction scheme has been studied and used for a long time, its study today is still of interest because of the high pressure on hydrocarbons prices all over the planet. Sharma *et al.* proposed a tool in the form of a comprehensive fixed-bed reactor model (2-dimensional, pseudo-homogeneous, gas–solid and steady state model) for FTS. The model is based on the main governing processes in terms of physical and chemical laws and considers internal mass transfer resistance. In their work it was shown that a foam catalyst allows better performances (activity per unit mass,  $C_{5+}$  selectivities and overall pressure drop) than packed extrudates, but at the expense of higher catalyst and reactor volumes. [12]. Turek *et al.* investigated low-temperature FTS over a CoRe/Al<sub>2</sub>O<sub>3</sub> catalyst in milli-structured fixed-bed reactors, experimentally and theoretically. They concluded that milli-structured fixed-bed reactors appear to be an interesting concept especially for small-scale FTS units [13]. In the recent years, by the high speed of computational calculations, Computational Fluid Dynamics (CFD) techniques have become a useful tool for simulation and analysis of variety of industrial problems that deal with fluid flow [14 - 16], heat and mass transfer [17 - 18] and chemical reactions [19 - 20]. By predicting a system's performance in various conditions, CFD can potentially be used to improve the efficiency of existing units as well as the design of new systems. It can help to shorten product and process development cycles, optimize processes to improve energy efficiency and environmental performance, and solve problems as they arise in plant operations. However, it is essential to validate the CFD results against data obtained from real operating systems. Krishna and Van Baten [21 - 22] employed CFD technique for describing hydrodynamics of bubble column reactors and its effects on scaling up this type of reactors. Jiang *et al.* [23] used a CFD approach for obtaining the detailed flow field and bubble behaviors in a novel two-stage fluidized bed reactor which was designed to produce diethyl oxalate from carbon monoxide based on the catalytic coupling reaction. A FTS microchannel reactor was modeled in three-dimensions by Arzamendi *et al.* [24]. They utilize a CFD model to analyze the effects of feed and cooling water flow rates and pressure on the performance of the reactor.

In our previous work, FTS fixed bed reactor based on Iron–zeolite catalyst was studied where in which use of saturated water as scraper of reaction heat was investigated. It was concluded that the temperature run away was controlled by utilizing saturated water, and the maximum temperature rising within the catalyst bed was 16K [25]. In the present work, a CFD model was developed to model FTS in a fixed bed nano-iron catalyst reactor. The catalyst bed was diluted in the entrance region of the bed in order to prevent hot spots. The thermodynamics properties of the gas mixture were calculated using Peng–Robinson equation of state [26]. The model predictions were validated with the measured data and the effect of operating conditions on the performance of the reactor were analyzed.

## 2. Material and methods

### 2.1. Process description

The employed reactor was a 1.2 cm diameter cylindrical reactor which was placed inside a heating jacket (Figure 1). The reactor included a preheating zone with 30cm height following by the reaction zone with 50cm height. It was designed and constructed by the Research Institute of Petroleum Industry, National Iranian Oil Company (RIPI-NIOC) in 2010 [27]. The reactor was packed with cylindrical Fe-SiO<sub>2</sub> catalysts (atomic ratios: 100Fe/5.64Cu/2La/19Si) with average diameter and length of 0.3 mm and 0.9 mm, respectively. The catalyst and bulk densities were 1290 and 730 kg/m<sup>3</sup>, respectively. The entrance region of the reaction section was diluted using ceramic particles in order to prevent the creation of hot spot. The experiments were run at different conditions of feed temperature, pressure, GHSV and H<sub>2</sub>/CO ratio as given in table 1.

Table 1 Operating conditions

Feed	543,563, 583 and	GHSV(hr <sup>-1</sup> )	1800, 5500,11000
Reactor	13,17,21 and 25	H <sub>2</sub> /CO molar ratio	0.5, 1,1.5 and 2

## 2.2. CFD modeling

### 2.2.1. Geometry and solution strategy

The reactor was modeled using a 1.2 cm × 80 cm axi-symmetric model. The computational domain was divided into 22,016 rectangular meshes was employed and the predicted profiles of temperature and species mole fractions were checked to be independent of the mesh size. The packed bed was considered as a porous media due to the large value of tube to catalyst diameter ratio ( $N > 12$ ) [28].

The entrance region of the reaction zone was considered as diluted reaction zone and the reaction rates in this zone were multiplied by catalyst/ (catalyst + ceramic) ratio. Mass-flow-inlet and pressure-outlet boundary conditions were used for reactor inlet and outlet, respectively. Constant temperature and no-slip condition was employed for the reactor walls. The finite volume method was used to discretize the partial differential equations of the model. The SIMPLE algorithm was employed for pressure-velocity coupling. The solution procedure is described in figure 2. The convergence criterion was based on the residual value of the calculated variables, namely mass, velocity components, and energy and species mass fractions. In the present calculations, the numerical computation was considered to be converged when the scaled residuals of the different variables were lower than  $10^{-4}$  for continuity and momentum equations and  $10^{-7}$  for the other variables.



Figure 1 FTS fixed-bed reactor

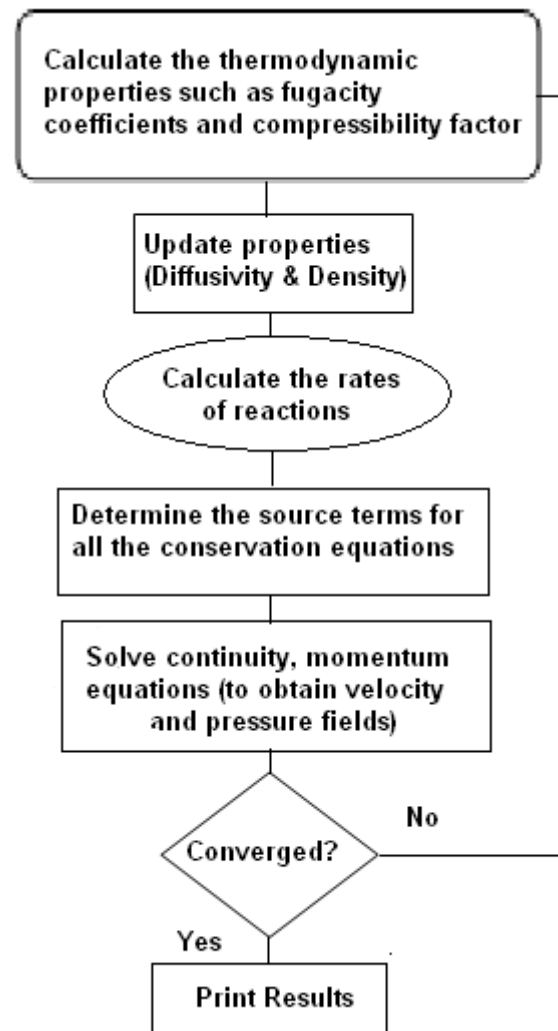


Figure 2. The solution procedure

### 2.2.2. Conservation equations

The mass conservation, momentum, energy and species, can be expressed as:

$$\text{Mass: } \nabla \cdot (\vec{v}\rho) = 0 \quad (1)$$

$$\text{Momentum: } \nabla \cdot (\rho \vec{v}\vec{v}) = -\nabla P + \nabla \cdot [\mu(\nabla \vec{v} + \nabla \vec{v}^T)] + \rho g + S \quad (2)$$

$$\text{Energy: } \nabla \cdot (\vec{v}(\rho H + P)) + \nabla \cdot \left( \sum_{i=1}^n h_i j_i \right) = -\nabla \cdot (q) + S_R \quad (3)$$

$$\text{Species: } \nabla \cdot (\vec{v}C_i - D_i \nabla C_i) = R_i \quad (4)$$

where,  $\rho$  represents mixture density,  $\vec{v}$  is velocity vector, H and  $h_i$  are total enthalpy and enthalpy of species, respectively. P is the static pressure and  $C_i$  stands for concentration of chemical species. The porous media of the reaction zone was modeled by addition of a momentum source term:

$$S = - \left( \sum_{j=1}^2 D_{ij} \mu v_j + \sum_{j=1}^2 C_{ij} \frac{1}{2} \rho |v| v_j \right) \quad (5)$$

The first term on the right-hand side of equation 5 is the viscous loss term the second term is the inertial loss term.  $|v|$  is the magnitude of the velocity and D and C are prescribed matrices. In this work, the flow in the reactor is laminar; therefore, the inertial term was ignored [29].  $S_R$  in equation (3) is the source of energy caused by chemical reaction:

$$S_R = - \left( \sum_j \frac{h_j^0}{M_j} R_j \right) \quad (6)$$

The temperature constant was defined at walls to establish isothermal condition at wall boundaries.

### 2.2.3. Physical properties

Peng-Robinson equation of state was used to predict the non-ideality [18] of the gas mixture:

$$\ln \hat{\phi}_i = (Z - 1) \frac{b_i}{b} - \ln(Z - \beta) - I \bar{q}_i, \quad q = \frac{a}{bRT}, \quad \bar{q}_i = q \left( 2 \times \frac{\frac{\partial a}{\partial x_i}}{a} - \frac{b_i [i]}{b} \right)$$

$$I = \frac{1}{\varepsilon_1 - \varepsilon_2} \ln \left( \frac{Z + \varepsilon_1 \times \beta}{Z + \varepsilon_2 \times \beta} \right), \quad \beta = \frac{bP}{RT}, \quad f_i = \hat{\phi}_i \times P \times y_i \quad (7)$$

$$b = \sum x_i b_i$$

where,  $f_i$  and  $\phi_i$  are species fugacity and fugacity coefficient respectively. R is the universal gas constant, M is the molecular weight of gas mixture and P is the operating pressure (taken to be 17 bar). b and beta are equation of state parameters. Z is the compressibility factor for calculation of the mixture density:

$$\rho = \frac{PM}{ZRT} \quad (8)$$

The parameters of equation (7) are listed in table 2. The specific heat of each species was defined as piecewise-polynomial function of temperature. Other thermal properties of the mixture such as molecular viscosity, thermal conductivity and diffusivity coefficient were calculated from Poling *et al.* [30].

Table2 Parameters of Peng-Rabinson EOS

$\sigma$	$\varepsilon$	$\Omega$	$\Psi$
$1 + \sqrt{2}$	$1 - \sqrt{2}$	0.07779	0.45724
$\alpha(T_r; \omega) = \left[ 1 + (0.37464 + 1.54226\omega - 0.26992\omega^2) \left( 1 - T_r^{1/2} \right) \right]^2$			
$Z = \beta + (Z + \varepsilon\beta)(Z + \sigma\beta) \left( \frac{1 + \beta - Z}{q\beta} \right), \quad \beta = \Omega \frac{P_r}{T_r}, \quad q = \frac{\alpha(T_r)\Psi}{\Omega T_r}$			

### 2.2.4. Reaction rate expressions

The considered reactions with 25 chemical species including CO, H<sub>2</sub>, CO<sub>2</sub>, H<sub>2</sub>O and C<sub>1</sub>-C<sub>21</sub> are listed in Table 3.

Table 3 List of FTS reactions

Num.	Reaction stoichiometry
1	$nCO + (n+1)H_2 \rightarrow C_nH_{2n+2} + nH_2O$
2	$CO + H_2O \rightarrow CO_2 + H_2$

The general form of rate equations [27] for production of C<sub>i</sub> is expressed as:

$$R_{C_i} = \frac{0.011 f_{H_2}^{0.7} f_{CO}^{-0.9}}{\left(2.2 - 0.18 \frac{f_{H_2}}{f_{CO}}\right)^{i-1}} \quad i = 4 - 9 \quad (10)$$

$$R_{C_i} = \frac{3 \times 10^{-5} f_{H_2}^{1.7} f_{CO}^{-1.1}}{\left(1.14 - 0.069 \frac{f_{H_2}}{f_{CO}}\right)^{i-1}} \quad i = 11 - 22 \quad (11)$$

$$R_{C_i} = .001518 * f_{H_2}^{0.241} / f_{CO}^{0.241} \quad (12)$$

$$R_{C_2} = .01819 * f_{H_2}^{0.045} / f_{CO}^{0.045} \quad (13)$$

$$R_{C_3} = .011 * f_{H_2}^{0.7} / f_{CO}^{0.9} \quad (14)$$

$$R_{C_{10}} = 3 \times 10^{-5} * f_{H_2}^{1.7} / f_{CO}^{1.1} \quad (15)$$

Reaction (2) is known as water-gas-shift (WGS) reaction and its rate [11] can be expressed as:

$$R_{WGS} = \frac{k_w \left( f_{CO} f_{H_2O} - \frac{f_{CO_2} f_{H_2}}{K_{WGS}} \right)}{\left( 1 + K_1 f_{CO} + K_2 f_{H_2O} \right)^2}$$

The kinetic parameters of WGS reaction rate are given in table 4 where,  $K_{WGS}$  is the equilibrium constant and can be calculated as follows:

$$\log K_{WGS} = \left( \frac{2073}{T} - 2.029 \right) \quad (16)$$

Table 4 Rates parameters for WGS reaction

Parameter	Value
$k_w$	0.21 mmol.g cat <sup>-1</sup> .S <sup>-1</sup> .bar <sup>-2</sup>
$K_1$	0.39 bar <sup>-1</sup>
$K_2$	3.54 bar <sup>-1</sup>

### 3. Results and discussion

Compressibility factor of the gas mixture is a criterion of its deviation from the ideal behavior. A contour plot of the predicted compressibility factor along the reactor is shown in figure 3. The figure shows that the formation of heavy hydrocarbons cause the compressibility factor to descend to about 0.9. Therefore, it is necessary to consider the mixture's non-ideality in calculation of density. A comparison between the predicted and measured values of C<sub>5+</sub> selectivity, CO conversion and temperature at three points (at beginning, middle and end of catalytic bed) along the reactor for two different operating conditions are given in table 5. The values in this table demonstrate that the error values are less than 4% for all of the compared variables. That is to say, the model in this work can successfully predict the performance of the fixed-bed FT process. Contour plots of temperature inside the reactor shown in figure 6 demonstrates that There is a temperature raise of about 17K in the beginning of the catalytic bed due to the high partial pressure of the

reactants and the high rate of exothermic reactions in this region. However, this amount of temperature raise is tolerable for this process and it could be claimed that the reactor was well controlled at the desired inlet temperature by dilution of the catalyst at the entrance of the reaction zone.

Table 5 Comparison between measured and predicted values for the bench-scale FTS processes

Beginning, middle and end of catalytic bed		Exp.	Pred.	%Error
GHSV=5500 hr <sup>-1</sup>	CO Conversion (%)	83	84.4	1.7
	C <sub>5+</sub> selectivity	32.4	32.5	0.3
T=563	Temperature at the beginning, of catalytic bed (K)	580	582	0.3
H <sub>2</sub> /CO=1	Temperature at the middle of catalytic bed (K)	575	576	0.2
P=17 bar	Temperature at the end of catalytic bed (K)	564	568	0.7
GHSV=5500 hr <sup>-1</sup>	CO Conversion (%)	93.2	94.6	1.5
	C <sub>5+</sub> selectivity	26.2	27	3.1
T=583	Temperature at the beginning, of catalytic bed (K)	595	589	-1.0
H <sub>2</sub> /CO=1	Temperature at the middle of catalytic bed (K)	590	573	-2.9
P=17 bar	Temperature at the end of catalytic bed (K)	584	582	-0.3

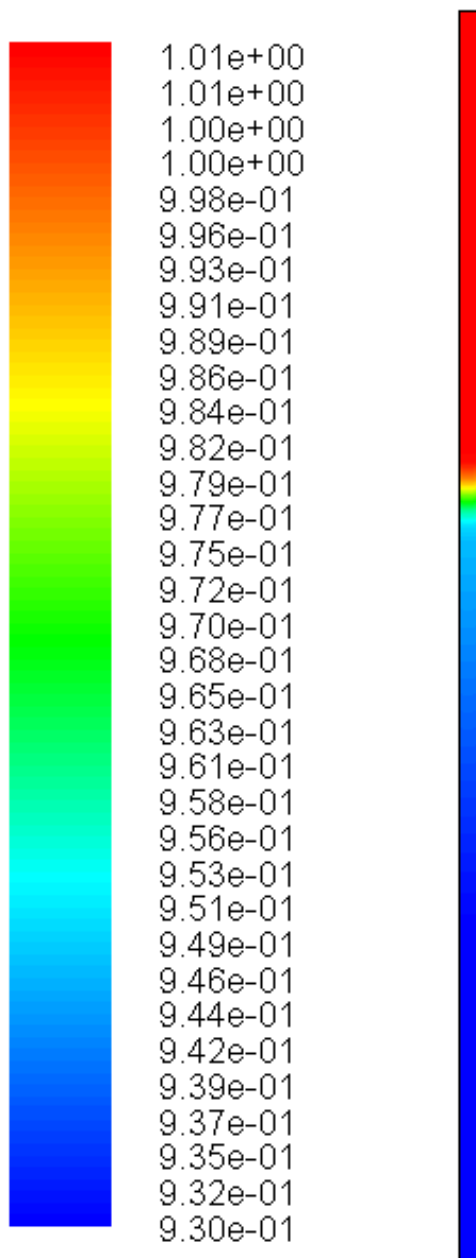


Fig. 3 Gas mixture compressibility factor (Z) contour along the reactor (T=573, P=17 bar, GHSV=5500 hr<sup>-1</sup> and CO/H<sub>2</sub>=1)

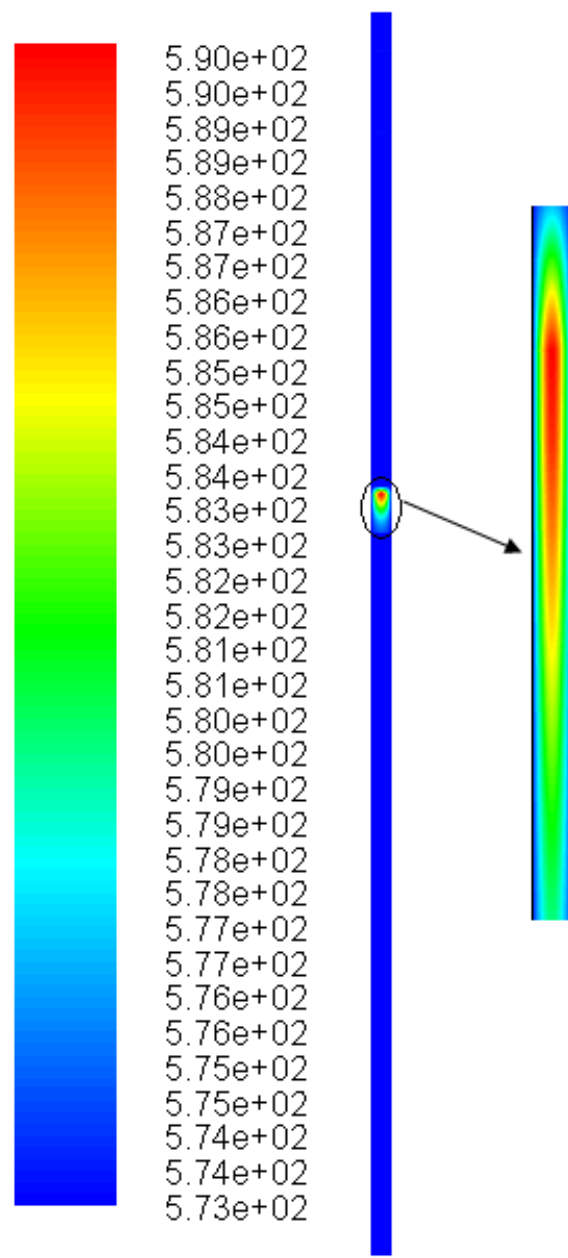


Fig. 4 Contour of temperature (T=573, P=17 bar, GHSV=5500 hr<sup>-1</sup> and CO/H<sub>2</sub>=1)

Profiles of species mass fraction along the reactor are plotted in figure 5. Concentrations of the reactants (CO and H<sub>2</sub>) are reduced due to their consumption along the reactor. Therefore, the reaction rates are reduced and consequently the slopes of species concentration curves along the reactor are decreased. The figure shows that the main changes in the concentrations of reactants and products occur in the beginning of the catalytic zone except for CO and ethane. Ethene acts as a monomer or building block during the FTS. Re-adsorption of ethene will result in a decrease of the ethane yield and an increase of higher hydrocarbons [31- 32]. This effect was included in ethane production rate (the power of CO and H<sub>2</sub> concentration in equation (12) is much less than that in other rate equations). The difference between the style of CO concentration profile and that of the other species can also be related to this effect. Figure 6 interprets the mixture density along the reactor. As it is expected, the mixture density increases along the reactor due to the formation of heavier hydrocarbons. The same reason can be used to describe the velocity reduction along the reactor as shown in figure 7. The parabolic radial velocity distribution (in the preheating zone) and zero velocity near the walls due to the non-slip wall boundary condition are also observed in this figure. In addition, pressure drop in the porous region causes the gas velocity to become almost uniform in the radial direction.

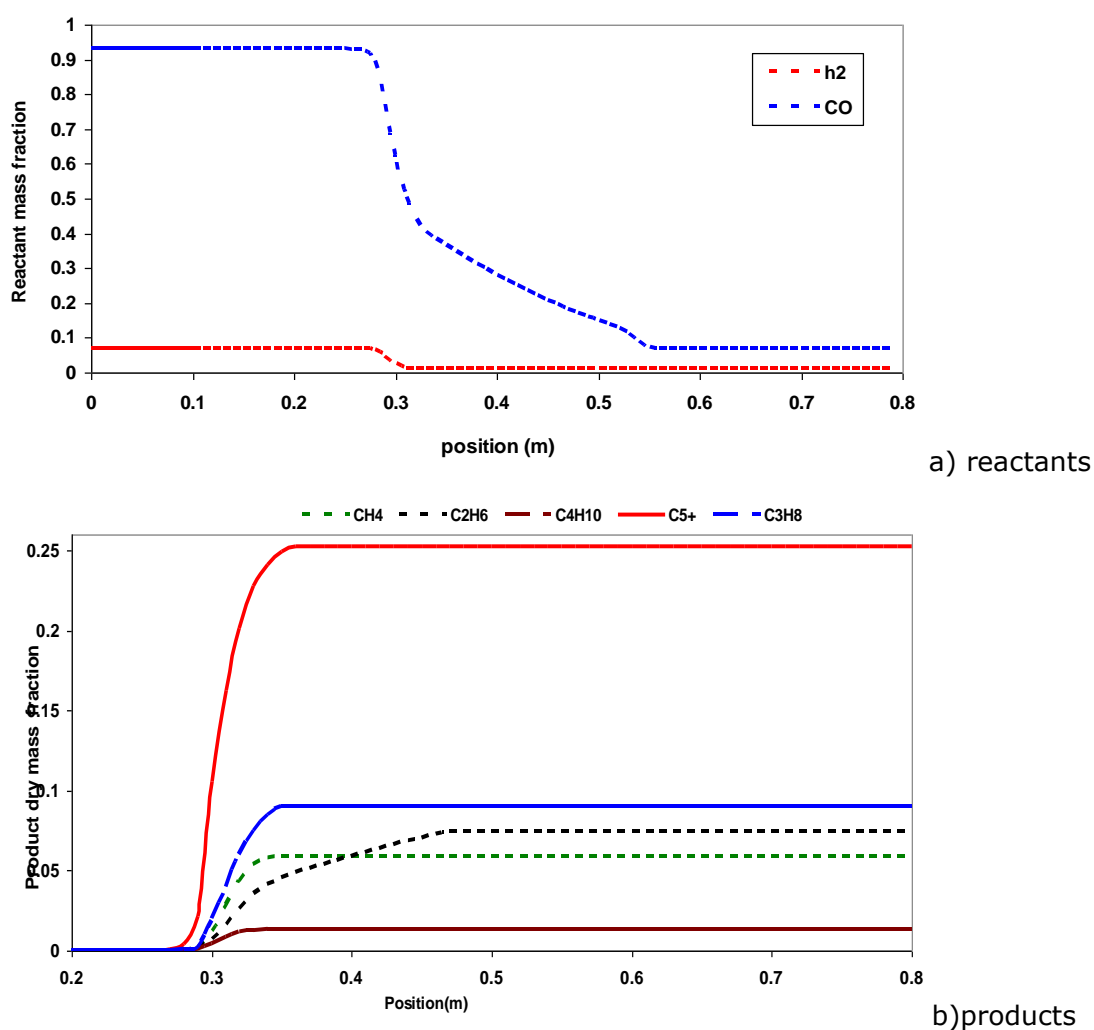


Fig. 5. Mass fraction of species along the reactor length ( $T=573$ ,  $p=17$  bar,  $\text{CO}/\text{H}_2=1$  and  $\text{GHSV}=5500 \text{ hr}^{-1}$ )

The reactor model was run at four different levels of each operating parameters (temperature, GHSV, pressure and H<sub>2</sub>/CO ratio) and the effects of these parameters on the performance of the reactor were investigated. In all cases, one parameter was changed and the other parameters were kept constant.

The effect of inlet temperature on C<sub>5+</sub> selectivity (g C<sub>5+</sub>/g converted feed) is shown in figure 8. This figure represents that increasing the temperature from 543 to 563 K increases the C<sub>5+</sub> selectivity. However, further increasing of the temperature to 583K decreases C<sub>5+</sub> selectivity. Increasing the reactor temperature has two opposite effects: it increases

the rate of reactions and on the other hand, it shifts the WGS equilibrium reaction into consumption of CO to produce CO<sub>2</sub>. When the reactor inlet temperature increases from 563 to 583K, the second effect is dominant and the production of C<sub>5+</sub> reduces due to the reduction in the concentration of CO.

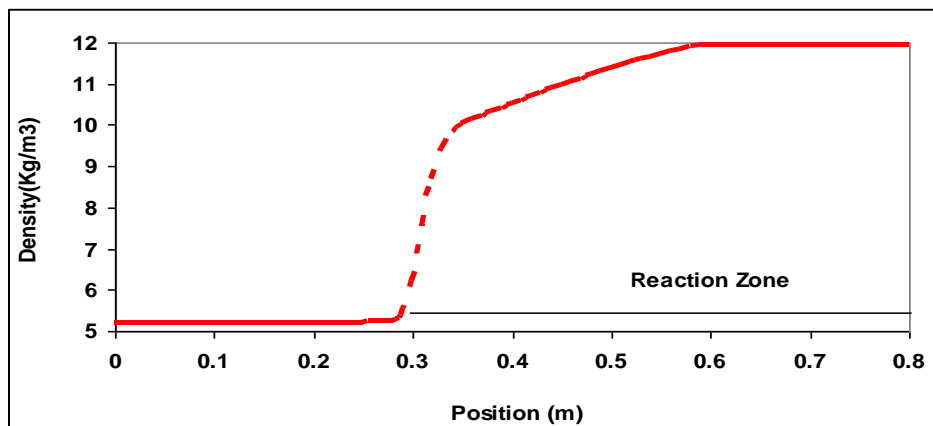


Figure. 10. Selectivity of C<sub>5+</sub> and CO conversion at different H<sub>2</sub>/CO molar: (T=573, P=17 bar and GHSV= 5500 hr<sup>-1</sup>)

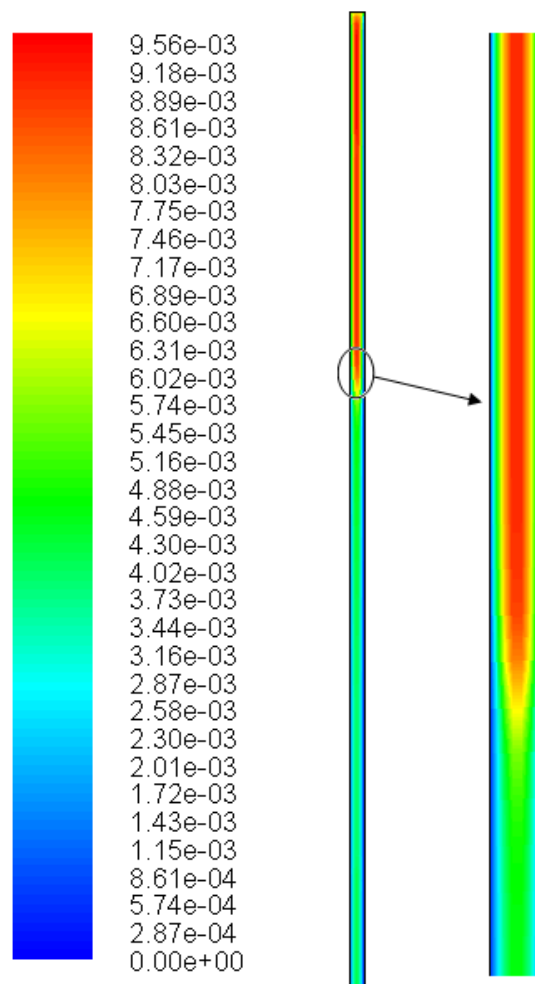


Figure.7: Contour of velocity (T=573, P=17 bar, GHSV=5500 hr<sup>-1</sup> and CO/H<sub>2</sub>= 1)

The effects of H<sub>2</sub>/CO molar ratio on C<sub>5+</sub> selectivity are presented in Figure.10. The figure interprets that although increasing the H<sub>2</sub>/CO ratio, raises the conversion of CO, but production of heavy hydrocarbons reduces. The former effect can be related to the fact that Hydrogen can participate in termination steps of polymerization reactions [31-33]. The effect of pressure as another important affecting parameter on this process is investigated in figure 11. According to this figure, the C<sub>5+</sub> selectivity increases by increasing total pressure to reach a maximum at a pressure of about 13 bars and thereafter, it takes a descending style. This can be explained by the fact that by increasing the total pressure, the partial pressures of reactants increase which results in increase of C<sub>5+</sub> and water as

products. The presence of water more than a threshold concentration, has a negative effect on  $C_{5+}$  selectivity [34]. Also the approximate values of optimum operating conditions in order to reach the maximum yield were obtained ( $P=21$  bar,  $T= 560$  K,  $GHSV=5700$  hr<sup>-1</sup> and  $H_2/CO=1$ ).

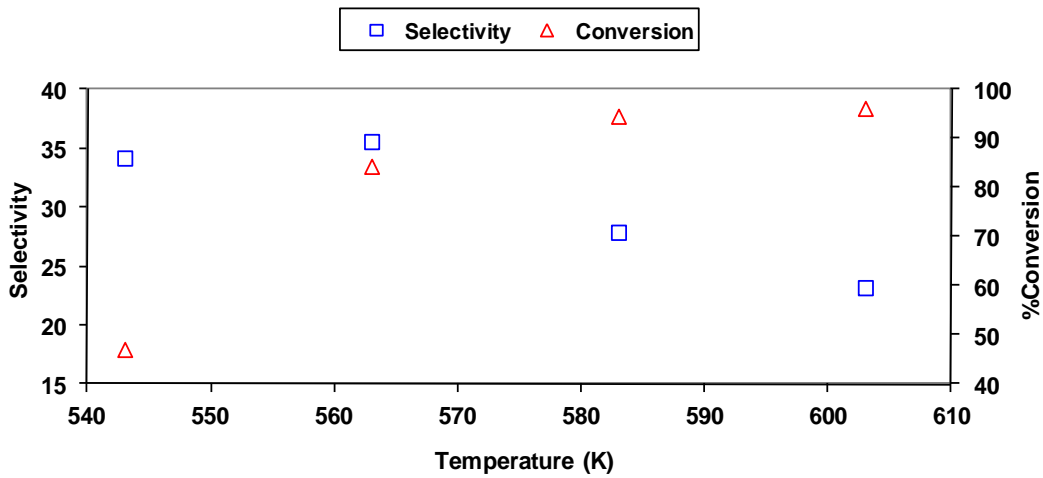


Figure. 8. Selectivity of  $C_{5+}$  and CO conversion at different temperatures ( $P=17$  bar,  $GHSV=5500$  hr<sup>-1</sup> and  $CO/H_2=1$ )

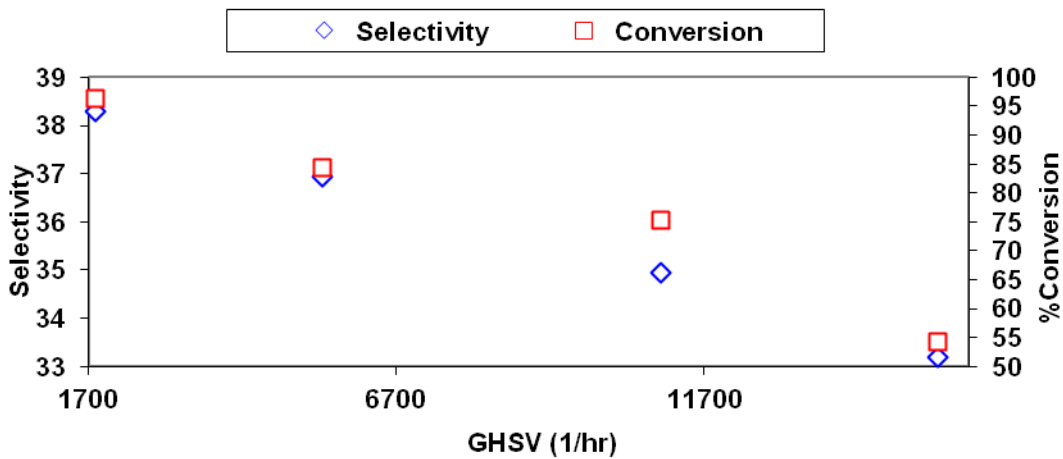


Figure. 9. Selectivity of  $C_{5+}$  and CO conversion at different GSHVs ( $T=573$ ,  $P=17$  bar and  $CO/H_2=1$ )

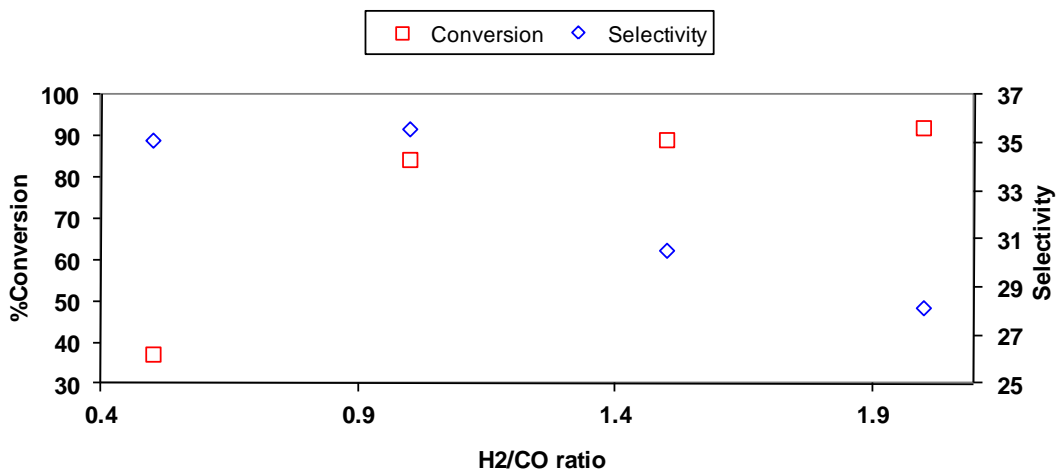


Figure. 10. Selectivity of  $C_{5+}$  and CO conversion at different  $H_2/CO$  molar: ( $T=573$ ,  $P=17$  bar and  $GHSV= 5500$  hr<sup>-1</sup>)

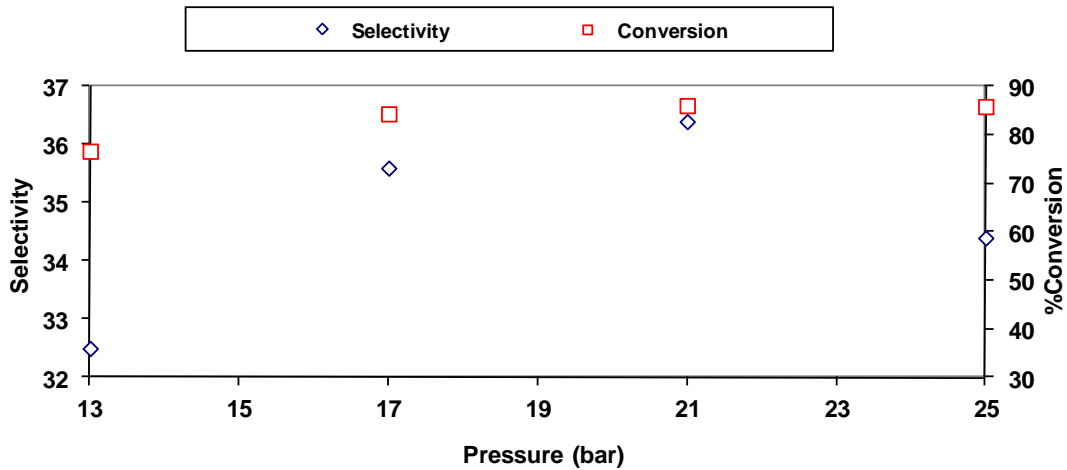
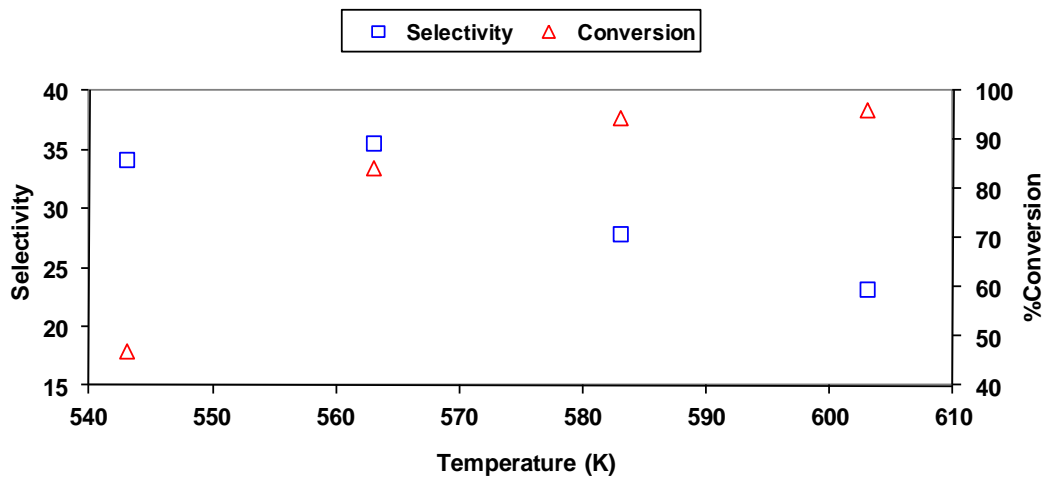


Figure. 11. Selectivity of  $C_{5+}$  and CO conversion at different pressures: ( $T=573$ ,  $GHSV=5500 \text{ hr}^{-1}$   $CO/H_2=1$  )



#### 4. Conclusions

Production of gasoline from Fischer–Tropsch Synthesis (FTS) process in a bench scale fixed-bed reactor was investigated using experiment and CFD modeling. Peng–Robinson equation of state was utilized to model the non-ideality of the gas mixture. The temperature raise at the beginning of catalytic bed was controlled by dilution of catalyst bed with ceramic particles. The simulation results were compared against the experimental data and good agreements were observed. The effects of operating conditions such as temperature, pressure, GHSV and  $H_2/CO$  ratio on reactor performance were studied using the validated model. The approximate values of optimum operating conditions in order to reach the maximum yield were obtained ( $P=21 \text{ bar}$ ,  $T= 560 \text{ K}$ ,  $GHSV=5700 \text{ hr}^{-1}$  and  $H_2/CO=1$ ). Since the model has proven to be in good agreement with the experimental data, it could be used in further studies to find more accurate values for the optimum conditions of temperature and GHSV without the need for hard experimental studies.

#### Nomenclature

P Pressure, bar	R Global Gas Factor, $\text{kJ.kmol}^{-1}.\text{K}^{-1}$
g gravity acceleration, $\text{m.s}^{-2}$	$M_i$ Molecular Weight, $\text{kg.kmol}^{-1}$
v velocity, $\text{m.s}^{-1}$	V Volume, $\text{m}^3$
H Total enthalpy, $\text{kJ.kg}^{-1}.\text{s}^{-1}$	$x_i$ mass fraction
h Enthalpy of species, $\text{kJ.kg}^{-1}.\text{s}^{-1}$	D Total Diffusivity Coefficient, $\text{m}^2.\text{s}^{-1}$
j Mass flux, $\text{kg.m}^{-2}.\text{s}^{-1}$	$k_m$ Thermal Conductivity, $\text{kJ.m}^{-1}.\text{K}^{-1}$
q Heat flux, $\text{kJ.m}^{-2}.\text{s}^{-1}$	
S Momentum source term,	
$D_{ij}$ Diffusivity coefficient,	

Ci Concentration, kmol.m<sup>3</sup>  
 Z Compressibility Factor  
 T Temperature, K  
 f fugacity, bar  
 ki Kinetic Constant, mol.hr<sup>-1</sup>.gr<sup>-1</sup>.bar<sup>-1</sup>  
 Ei Activation Energy, kJ.kmol<sup>-1</sup>  
 Beta EOS parameter  
 q EOS parameter

#### Greek Letters

$\rho$  Density, kg.m<sup>-3</sup>  
 $\mu$  Viscosity, kg.m<sup>-1</sup>.s<sup>-1</sup>  
 $\varphi_i$  Fugacity coefficient

#### Subscript

i species number  
 j second species number  
 m mixture

#### References

- [1] H. Schulz, Short history and present trends of Fischer–Tropsch Synthesis, Appl. Catal. A-Gen.186 (1999) 3-12.
- [2] M.E.Dry, The Fischer–Tropsch process: 1950–2000. Catal. Today .71 (2002), 227-241.
- [3] J.B. Butt, T. Lin, L.H. Schwartz, Iron alloy Fischer-Tropsch catalysts. VI. FeCo on ZSM-5, J. Catal.97 (1986)261-263.
- [4] H. Schulz, H.L. Niederberger, M. Kneip, F. Weil, Synthesis Gas Conversion on Fischer-Tropsch Iron/HZSM5 Composite Catalysts, Stud. Surf. Sci Catal.61 (1991) 313-323.
- [5] G. Calleja, A.D. Lucas, R.V. Grieken, Co/HZSM-5 catalyst for syngas conversion: influence of process variables, Fuel.74 (1995) 445-451.
- [6] A.P. Steynberg, M.E. Dry, B.H. Havis, B.B. Berman, Chapter 2 Fischer-Tropsch Reactors, Stud. Surf. Sci Catal.152 (2004)64.
- [7] Q.S. Liu, Z.X. Zhang, J.L. Zhou, Steady state and dynamic behaviour of fixed bed catalytic reactor for Fischer-Tropsch synthesis. I. mathematical model and numerical method, J. Nat.Gas .Chem, 8 (1999) 137-180.
- [8] Q.S. Liu, Z.X. Zhang, J.L. Zhou, Steady state and dynamic behaviour of fixed bed catalytic reactor for Fischer-Tropsch synthesis. II. Steady state and dynamic simulation results, J.Nat.Gas .Chem, 8 (1999) 238-265.
- [9] Y. Wang, Y. Xu, Y. Li, Y. Zhao, B. Zhang, Heterogeneous modeling for fixed-bed Fischer–Tropsch synthesis: Reactor model and its applications, Chem. Eng. Sci. 58 (2003) 867-875.
- [10] M.R. Rahimpour, S.M. Jokar, Z. Jamshidnejad, A novel slurry bubble column membrane reactor concept for Fischer–Tropsch synthesis in GTL technology, Chem. Eng. Res. Des. (2011) In Press.
- [11] A. Nakhaei Pour, M.R. Housaindokht, S.F. Tayyari, J. Zarkesh, S.M Kamali Shahri, Water-gas-shift kinetic over nano-structured iron catalyst in Fischer-Tropsch, J. Nat.Gas. Sci. Eng. 2(2010) 79-85.
- [12] A. Sharma, R. Philippe, F.Luck, D.Schweich, A simple and realistic fixed bed model for investigating Fischer–Tropsch catalyst activity at lab-scale and extrapolating to industrial conditions, Chem. Eng.Sci. 66(2011) 6358-6366.
- [13] J. Knochen, R. Güttel, C. Knobloch, T.Turek, Fischer–Tropsch synthesis in milli-structured fixed-bed reactors: Experimental study and scale-up considerations, Chemical Engineering and Processing 49 (2010) 958–964.
- [14] X.G. Li, D. X. Liuc, S.M Xu, H. Li, CFD simulation of hydrodynamics of valve tray, Chemical Engineering and Processing 48 (2009) 145–151.
- [15] S. Vashisth, K.D.P. Nigam, Prediction of flow profiles and interfacial phenomena for two-phase flow in coiled tubes, Chemical Engineering and Processing 48 (2009) 452–463.
- [16] A.I. Stamou, Improving the hydraulic efficiency of water process tanks using CFD models, Chemical Engineering and Processing 47 (2008) 1179–1189.
- [17] M. Rahimi, S.R. Shabanian, A.A. Alsairafi, Experimental and CFD studies on heat transfer and friction factor characteristics of a tube equipped with modified twisted tape inserts, Chemical Engineering and Processing 48 (2009) 762–770.
- [18] M. Irani, R.B. Bouzarjomehri, M.R. Pishvaei, Impact of thermodynamic non-idealities and mass transfer on multi-phase hydrodynamics, Scientia Iranica 17 (2010) 55-64.
- [19] M. Irani, A. Alizadehdakhel, A. Nakhaei Pour, N. Hoseini, M. Adinehnia, CFD modeling of hydrogen production using steam reforming of methane in monolith reactors: Surface or volume-base reaction model? Int. J. Hydrogen. Energ.

- 36(2011)15602-15610.
- [20] B. Chalermsoosuan, P. Kuchonthara, P. Piumsomboon, Effect of circulating fluidized bed reactor riser geometries on chemical reaction rates by using CFD simulations, *Chemical Engineering and Processing* 48 (2009) 165–177.
- [21] R. Krishna, J.M. Van Baten, Scaling up bubble column reactors with the aid of CFD, *Chem. Eng. Res. Des.* 79(2001) 283-309.
- [22] J.M. Van Baten, R. Krishna, Scale Effects on the Hydrodynamics of Bubble Columns Operating in the Heterogeneous Flow Regime, *Chem. Eng. Res. Des.* 82(2004) 1043-1053.
- [23] C.W. Jiang, Z.W. Zheng, Y.P. Zhu, Z.H. Luo, Design of a two-stage fluidized bed reactor for preparation of diethyl oxalate from carbon monoxide, *Chem. Eng. Res. Des.* (2011) In press.
- [24] G. Arzamendi, P.M. Diéguez, M. Montes, J.A. Odriozola, E.F. Sousa-Aguiar, L.M. Gandía, Computational fluid dynamics study of heat transfer in a microchannel reactor for low-temperature Fischer–Tropsch synthesis, *Chem. Eng J.* 160 (2010) 915–922.
- [25] M. Irani, A. Alizadehdakhl, A. Nakhaeipour, P. Prolx, A. Tavassoli, An investigation on the performance of a FTS fixed-bed reactor using CFD methods, *Int. Commun. Heat. Mass.* 38(2011) 1119–1124.
- [26] M. Irani, R.B. Bozorgmehry, M.R. Pishvaie, A. Tavassoli, Investigating the Effects of Mass Transfer and Mixture Non-Ideality on Multiphase Flow Hydrodynamics using CFD Methods, *Iran. J. Chem. Eng.* 29 (2010) 51-60.
- [27] A. Nakhaei Pour, M.R. Housaindokht, S. F. Tayyari, J. Zarkesh, Effect of nano-particle size on product distribution and kinetic parameters of Fe/Cu/La catalyst in Fischer-Tropsch synthesis, *J. Nat. Gas. Chem.* 19(2010)107–116.
- [28] E. A. Foumeny, H. A. Moallemi, C. Mcgreavy, J. A. A. Castro, Elucidation of mean voidage in packed beds, *Can. J. Chem. Eng.* 69 (2010)1010-1015.
- [29] Fluent, Incorporated: FLUENT 6 USER Manual, Lebanon (NH): Fluent Inc., 2001.
- [30] B.E. Poling, J.M. Prausnitz, J.P. O’Connell, *The properties of gases & liquids*, 5th ed. McGraw-Hill, New York, 2000.
- [31] S. Novak, R. J. Madon, and H. Suhl, Secondary effects in the Fischer-Tropsch synthesis, *J. Catal.* 77(1982) 141.
- [32] B. Sarup and B.W. Wojciechowski, Studies of the fischer-tropsch synthesis on a cobalt catalyst i. evaluation of product distribution parameters from experimental data, *Can. J. Chem. Eng.* 66(1988) 831.
- [33] G.P. Van der Laan, A. A. C. M. Beenackers, Kinetics and Selectivity of the Fischer-Tropsch Synthesis: A Literature Review, *Catalysis Reviews, CATAL. REV. SCI. ENG.* 41(1999), 255–318.
- [34] S. Krishnamoorthy, A. Li, E. Iglesia, Pathways for CO<sub>2</sub> Formation and Conversion During Fischer–Tropsch Synthesis on Iron-Based Catalysts, *Catal. Lett.* 80 (2002)77-86.

---

*Corresponding author, PhD of Chemical Engineering. postal address: Gas Division, Research Institute of Petroleum Industry (RIPI), West Blvd., Near Azadi Sports Complex, Tehran, Iran, Phone: +98 (21) 48252403, Fax: +98 (21) 44739716 E-mail address: [Iranim@ripi.ir](mailto:Iranim@ripi.ir) or [Mohammadirani@yahoo.com](mailto:Mohammadirani@yahoo.com)*